
Proceedings Paper:
Worley, R. orcid.org/0000-0002-3607-2650, Yu, Y. and Anderson, S. orcid.org/0000-0002-7452-5681 (2020) Acoustic echo-localization for pipe inspection robots. In: 2020 IEEE International Conference on Multisensor Fusion and Integration for Intelligent Systems (MFI). 2020 IEEE International Conference on Multisensor Fusion and Integration for Intelligent Systems (MFI), 14-16 Sep 2020, Karlsruhe, Germany. Institute of Electrical and Electronics Engineers (IEEE) , pp. 160-165.

https://doi.org/10.1109/mfi49285.2020.9235225

Acoustic Echo-Localization for Pipe Inspection Robots

Rob Worley[1], Yicheng Yu[2], Sean Anderson[1]

Abstract— **Robot localization in water and wastewater pipes is essential for path planning and for localization of faults, but the environment makes it challenging. Conventional localization suffers in pipes due to the lack of features and due to accumulating uncertainty caused by the limited perspective of typical sensors. This paper presents the implementation of an acoustic echo based localization method for the pipe environment, using a loudspeaker and microphone positioned on the robot. Echoes are used to detect distant features in the pipe and make direct measurements of the robot's position which do not suffer from accumulated error. Novel estimation of echo class is used to refine the acoustic measurements before they are incorporated into the localization. Finally, the paper presents an investigation into the effectiveness of the method and the robustness of the method to errors in the acoustic measurements.**

I. INTRODUCTION

Water supply and wastewater pipes are in need of constant maintenance. This maintenance is costly, and would be improved by more precisely locating faults in the pipe network. Current location methods are inefficient, requiring manual inspection from above ground or using remotely controlled robots. These methods might be improved by using autonomous robots for persistent, pervasive inspection of a pipe network. These robots would be small, with limits on the size, power requirement, and cost of hardware.

Localization is important for pipe-inspection robots as it allows for effective path planning and for the location of faults to be accurately returned to an operator. However, this environment is challenging for localization. The environment restricts the use of typical robot sensors such as GPS and magnetic compasses [1], and vision-based localization is challenging due to feature sparseness [2], and due to the limited perspective in a pipe causing accumulated error from the integration of the uncertain relative position estimates made between images with little overlap in content.

A number of in-pipe robot localization methods have been demonstrated including the use of visual odometry [2], [3], [4], visual feature recognition [5], [6], and inertial [7], [8], [9], magnetic [1], and acoustic [10] sensing. These show a number of approaches to measuring aspects of the robot's state which could be used in sensor fusion.

Few investigations have been made into direct estimation of the position of the robot relative to distant features in a pipe beyond the view of a camera, which would reduce limits on the robot's perspective.

The use of an artificial field such as a radio signal in a pipe [11] has been shown, but it requires a separate transmitter, limiting the flexibility of the system in this application. The use of time of arrival (TOA) of acoustic signals has been demonstrated for in-pipe robots [12], where the delay arrival of an acoustic signal is used to estimate the distance travelled by the robot. However, in this case the robot is tethered to the sound source so that the delay in arrival can be measured, limiting the desired autonomy. To circumvent this, a loudspeaker can be positioned on the robot, allowing the measurement of TOA of acoustic echoes. This can give an absolute estimate of the position of features relative to the robot which does not suffer from accumulated error.

A number of methods for acoustic robot localization have been demonstrated. Recent work has used the direction of arrival of sounds from moving sources [13]. Other recent work has demonstrated the use of a single co-located acoustic source and receiver to estimate the position of a robot in a structured room [14], [15]. These methods use the *room impulse response* from a room with reflective walls to iteratively estimate a moving robot's position, the former using Bayes filtering and incorporating knowledge of the robot's motion, and the latter using optimization. These methods have been developed for multi-walled rooms where multi-path echoes are not considered and where it is assumed that each detected echo can be associated with a specific wall. However, the reflective pipe environment differs as multi-path echoes are observed and data association is challenging due to uncertainty in the echo measurements.

The measurement of acoustic echoes may be challenging in this application due to acoustic dispersion and the presence of environmental noise from flowing water and robot motion. Estimation of impulse responses in the presence of uncertainty has been done by finding acoustic model parameters that minimize the error between the predicted and measured impulse response [16].

This paper presents a method of acoustic echo-based localization for a robot moving through a pipe without a tether, which is demonstrated using experimental data. The incorporation of multi-path echoes is presented along with robust data association for measurements. The main novel contributions of this paper are a method of classifying the acoustic echoes by robustly estimating the length of the pipe (in Section II-D.2), required for removing undesired measurements, and the analysis of the sensitivity of the localization method to spurious or missing measurements (in Section III).

*R. Worley is supported by an EPSRC Doctoral Training Partnership Scholarship

[1]R. Worley and S. Anderson are with Department of Automatic Control and Systems Engineering, University of Sheffield, Sheffield, UK rfworley1@sheffield.ac.uk

[2]Yu, Y. is with Department of Mechanical Engineering, University of Sheffield, Sheffield, UK

Fig. 1. A photograph of the pipe used to record experimental data, and an illustration of the robot within a pipe emitting a sound which echoes from the ends of the pipe. Three different scenarios are shown, which have been created experimentally. In all cases one end is open, and in each case the other end is open, closed, or filled with absorber, respectively.

II. METHODS

A. Problem Definition

The robot moves along the axis of a pipe by a known input u_k to position x_k at time k with the state-space model

$$x_k = x_{k-1} + u_k + w_k \tag{1}$$

where additive normally distributed noise w_k is added to u_k at each step. This models the uncertainty in motion along the axis of the pipe due to obstruction to motion such as debris and due to unmeasured motion off the axis of the pipe. The aim is to estimate x_k in the presence of noise w_k.

After moving, the robot stops and makes an acoustic measurement. It is assumed that the robot is in an isolated pipe of unknown length which has acoustically reflective ends. The robot has a co-located loudspeaker and microphone so it can emit and receive a sound, as illustrated in Fig. 1, and use the measured impulse response to estimate the distances to the ends of the pipe. These measurements are used for localization, estimating the robot's position x_k and the positions of the ends of the pipe.

B. Acoustic Signal Processing

When the loudspeaker transmits an acoustic signal, the received signal is modelled in discrete time [17] by

$$r(t) = s(t) * h_x(t) = \sum_{z=0}^{t} s(z) h_x(t-z) \tag{2}$$

where the received signal r at time index t is given by the convolution of the transmitted signal s and the pipe transfer function between the loudspeaker and microphone at robot position x through the pipe, h_x.

An impulse with sufficient energy is difficult to produce using a small loudspeaker. Therefore the impulse response is not found directly but instead by using deconvolution, as the response is equal to the transfer function

$$H_x(\omega) = \frac{R(\omega)}{S(\omega)} \tag{3}$$

where each term is the Fourier transform of each corresponding term in Equation 2. This allows a chirp signal to be used, which has energy across a band of the frequency spectrum.

The impulse response is expected to be a series of impulses corresponding to each path an acoustic wave can take from source to receiver [15], [16], [18]. This is represented as

$$h_x(t) = \sum_{n=1}^{N} g_n \delta(t - \tau_n) \tag{4}$$

where there are N components, each of which is a Dirac delta impulse where the n^{th} component has magnitude g_n and delay τ_n.

A band-pass filter is applied to $r(t)$ and $s(t)$ to remove the effect of higher frequency dispersive wave effects and low frequency oscillation in the impulse response, allowing detection of each impulse component. This filtering adds delay which is removed using cross-correlation between the filtered pipe impulse response and the impulse response of the filter itself, and oscillation which is removed using envelope detection.

The signal processing is illustrated in Fig. 2(a), where the time delay τ_n has been converted to a distance to the source of reflection ξ_n by

$$\xi_n = \frac{1}{2} c \tau_n \tag{5}$$

where c is the wave speed. It is assumed that the wave speed is known, requiring calibration in the case of operation in varying temperature and humidity.

C. Experimental Acoustic Measurements

Fig. 2(b) shows the response found from measurements made in the 15 metre pipe seen in Fig. 1, where the robot is 1.5 metres from one end. Fig. 2(c) shows the estimated impulse response in the form of Equation 4, from which measurements ξ_n can be taken.

The first impulse corresponds to the direct path between the source and receiver, and is ignored in the subsequent methods. The second and third impulses correspond to first order echoes from the ends of the pipe. Fig. 2(d) shows that as the robot moves, these impulses move accordingly, so can be used as measurements of map features in localization.

The fourth impulse corresponds to the path equal to twice the length of the pipe, giving a distance to the reflection source equal to the pipe length, 15 metres. In Fig. 2(d) an impulse at this distance is seen for every robot position, so is a *static* measurement which, if used in the same way as the other measurements, would incorrectly appear to correspond to a feature which varies in position.

The further impulses correspond to the first order echo signals which have then travelled the path of the *static* measurement, adding a further delay equal to the length of the pipe. The multiple order echoes are simply offset in distance by multiples of the length of the pipe. Therefore, they could be used as direct measurements of the positions of the echo sources if the offset can be detected and removed, or as measurements of position of fictional echo sources outside the pipe. In this work, the latter approach is used.

If the robot is large enough with respect to the pipe, there may be significant acoustic reflection from it, which will result in echoes that appear to have travelled twice the

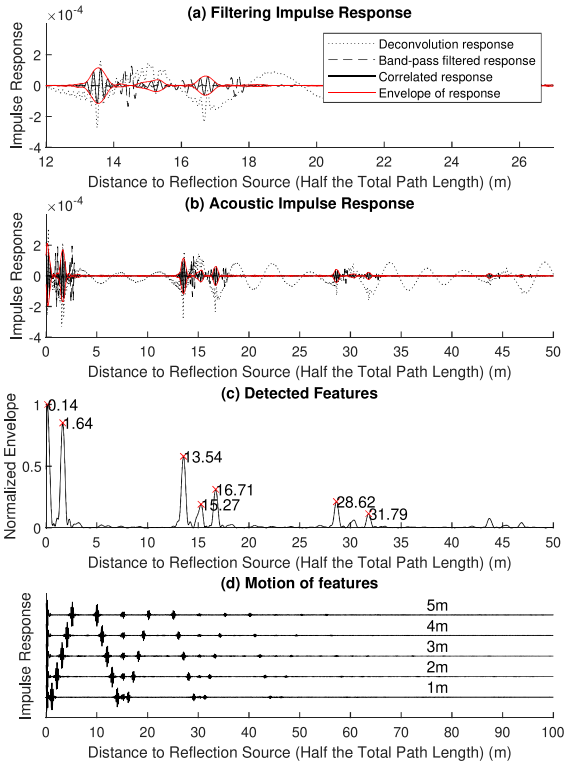

Fig. 2. The acoustic signal processing used to estimate the distances to reflective features in the pipe from the robot. (a) The signal processing sequence: Deconvolution is used to find the impulse response between the loudspeaker and microphone. A band-pass filter removes low frequency oscillation and high frequency diffuse wave effects. Cross-correlation and envelope detection are used to remove the offset and oscillation caused by the filtering. (b) The processed impulse response when the robot is 1.5 metres from an end of a 15 metre long pipe. (c) The envelope of the filtered impulse response. The detected impulses are labelled with their corresponding distance. (d) A set of experimental data showing the impulse response as the system moves through the pipe in steps of 1 metre. The position at which each impulse response was found is labelled. The amplitude is arbitrary, and the impulses are shown offset in amplitude.

distance to the feature. It is assumed that these echoes are able to be removed from the set of measurements, either by using a similar method to that described in section II-D.2, or by also using the amplitude of the impulse component, which will be smaller in this case.

Further processing is needed to use these measurements, desired and undesired, for robot localization.

D. Robot Localization

The measurements ξ_n will be subject to additive noise, and spurious or missing measurements are expected. With only one microphone there is only information about distance to features and not direction. Due to the uncertain and limited measurements the robot must combine multiple measurements in order to give a robust unique position estimate. This is formulated as an optimization problem in related work [15] using impulse measurements only. However, in a pipe a set of impulse responses cannot uniquely identify a trajectory. Therefore, information about the robot's motion must be incorporated into the localization, as in related work using Bayes filtering [14].

In this work, the Bayes filter is implemented as a Kalman filter [19], fusing acoustic measurements with the state space model, giving robustness to measurement noise and motion noise. Other implementations could also be applied, however the Kalman filter is suitable as the system is well modelled as linear with Gaussian noise, and the estimate is expected to be unimodal as ambiguities in sensing are resolved immediately.

The state to be estimated is defined as $\mathbf{y}_k = \begin{bmatrix} x_k & p_1 & p_2 & \dots & p_m & \dots & p_M \end{bmatrix}^T$, where x_k is the robot's position at time k, and p_m is the position of the m^{th} echo source, where there are M estimated echo sources. The sources of multiple order echoes are modelled as features at positions further than the ends of the pipe, as they appear to be in a fixed position like the sources of first order reflections. The state space model is therefore expanded from that in Equation 1, and is given by

$$\mathbf{y}_k = \mathbf{A}\mathbf{y}_{k-1} + \mathbf{u_k} + \mathbf{w_k} = \mathbf{I}\mathbf{y}_{k-1} + \begin{bmatrix} u_k \\ 0 \\ \vdots \\ 0 \end{bmatrix} + \begin{bmatrix} w_k \\ 0 \\ \vdots \\ 0 \end{bmatrix} \tag{6}$$

The estimate is parameterized as a Gaussian distribution over each state dimension with mean $\boldsymbol{\mu}_k$ and covariance matrix $\boldsymbol{\Sigma}_k$. This estimate is initialised as $\boldsymbol{\mu}_0 = \begin{bmatrix} x_0 & p_1 \end{bmatrix}^T = \begin{bmatrix} 0 & 0 \end{bmatrix}^T$ when the robot is at one end of the pipe. The size of this vector is increased as measurements are made and the estimated number of echo sources increases. Apart from the defined echo source at position p_1, estimated echo sources that are not observed for a number of time steps are removed from the estimation and the state is resized accordingly.

At each time k, the robot moves, finds the acoustic impulse response as a set of N_k distance measurements $\xi_k = \{\xi_{1,k} \quad \xi_{2,k} \quad \dots \quad \xi_{N_k,k}\}$, and performs the following two functions to update the localization estimate.

1) Estimate State: The Kalman filter uses the acoustic measurements ξ_k and pipe length estimate $\hat{\Lambda}_k$ to update the estimate of state $\mathbf{y}_k$. Two filter steps are required at each time step. The prediction step propagates the state estimate through the state-space model. The predicted mean and covariance are given by

$$\bar{\boldsymbol{\mu}}_k = \mathbf{A}\boldsymbol{\mu}_{k-1} + \boldsymbol{u}_k \tag{7}$$

$$\bar{\boldsymbol{\Sigma}}_k = \mathbf{A}\boldsymbol{\Sigma}_{k-1}\mathbf{A}^T + \mathbf{R}_k \tag{8}$$

where $\mathbf{R}_k$ is the motion uncertainty matrix. The update step is computed firstly for the pipe length estimate and then separately for each acoustic measurement.

Only the distance corresponding to each acoustic measurement is known, not the direction. Therefore, data association is computed for both positive and negative displacements for each distance measured, giving $I_k = 2N_k$ measurements.

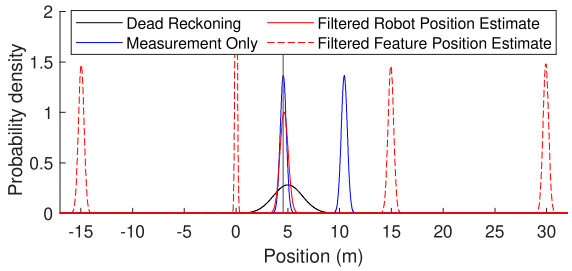

Fig. 3. An illustration of the function of the robot localization method in a 15 metre pipe. Two values are seen from the measurement-only estimate. The multivariable output from the Kalman filter is shown with a single robot position estimate and multiple feature position estimates.

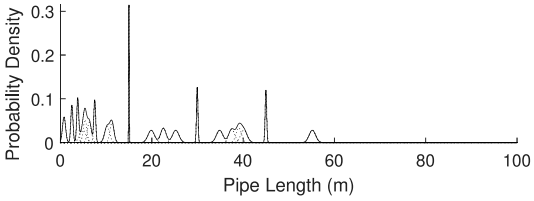

Fig. 4. An illustration of a measure of the probability distribution of possible pipe lengths given a number of measurement sets in a 15 metre pipe. The multimodal probability distribution defined as a sum of Gaussian distributions each parameterised by a mean and variance. It can be seen that the most likely estimated length is correct, and that other likely length estimates correspond to multiples of the pipe length.

At each time index k, for each of these measurements i, for each of the existing features m, a data association value $\pi_{i,m,k}$ equal to the Mahalanobis distance [19] is computed by

$$\Psi_{i,m,k} = \mathbf{C}_m \bar{\mathbf{\Sigma}}_k \mathbf{C}_m^T + Q_k \tag{9}$$

$$\pi_{i,m,k} = (\xi_{i,k} - \bar{\xi}_{m,k})^2 \Psi_{i,m,k}^{-1} \tag{10}$$

$\mathbf{C}_m$ is the output vector for the robot position and the feature m, equal to $\begin{bmatrix}1 & 0 & \dots & 0 & -1 & 0 & \dots & 0\end{bmatrix}$ or $\begin{bmatrix}-1 & 0 & \dots & 0 & 1 & 0 & \dots & 0\end{bmatrix}$ depending on the direction of $\bar{p}_m$ from $\bar{x}_k$, and their relative positions in the vector $\boldsymbol{\mu}_k$. Q_k is the measurement uncertainty parameter, used to give a measure of the feature's covariance $\Psi_{i,m,k}$. $\pi_{i,m,k}$ is the data association value computed using the i^{th} measurement $\xi_{i,k}$ and the expected measurement for feature m, $\bar{\xi}_{m,k}$.

The smallest value of π is found. If it is larger than a threshold, a new feature is created. If it is smaller than the threshold, the corresponding feature j and measurement direction are used to compute the Kalman filter update using

$$\mathbf{K}_{i,j,k} = \bar{\mathbf{\Sigma}}_k \mathbf{C}_j^T \Psi_{i,j,k}^{-1} \tag{11}$$

$$\bar{\boldsymbol{\mu}}_k = \bar{\boldsymbol{\mu}}_k + \mathbf{K}_{i,j,k}(\xi_{i,k} - \bar{\xi}_{j,k}) \tag{12}$$

$$\bar{\mathbf{\Sigma}}_k = (\mathbf{I} - \mathbf{K}_{i,j,k}\mathbf{C}_j)\bar{\mathbf{\Sigma}}_k \tag{13}$$

These Kalman filter steps are repeated at each time step to estimate the state $\mathbf{y}_k$ using the set of measurements ξ_k. For the measurement $\hat{\Lambda}_k$, the equivalent to Equation 12 is

$$\bar{\boldsymbol{\mu}}_k = \bar{\boldsymbol{\mu}}_k + \mathbf{K}_{m,k}(\hat{\Lambda}_k - p_{m,k}) \tag{14}$$

where p_m is the position of feature at the other end of the pipe from p_1.

An illustration of the function of the Kalman filtering is shown in Fig. 3. The probability distribution estimated for each component of the state $\mathbf{y}_k$ is shown. Estimated features positioned at multiples of the pipe length can be seen, as expected given the definition of $\mathbf{y}_k$. The *dead reckoning* estimate, using only the initial velocity, is shown to have a large variance. The *measurement-only* estimates are shown to give accurate distances to the end of the pipe but are unable to estimate which measurement corresponds to which end, giving two estimates of position.

2) Estimate Echo Class: It is desired to classify a measurement as either corresponding to a first or multiple order reflection from a pipe feature, or corresponding to a multiple of the pipe length. This has two purposes: Firstly, the static measurement corresponding to the pipe length can be removed from the set ξ_k as it is detrimental to the localization estimate. Secondly, the estimate of the pipe length can be used as a virtual measurement between the features at each end of the pipe, which can improve the localization estimate. This is done by estimating the pipe length from the acoustic measurements.

For pipe length Λ, given uncertainty in the measurements, the pipe length estimate $\hat{\Lambda}_k$ is described as a probability distribution $p(\Lambda|\xi_1, \xi_2, \dots, \xi_k) = p(\hat{\Lambda}_k|\xi_1, \xi_2, \dots, \xi_k)$, which is the probability of pipe length estimate $\hat{\Lambda}_k$ given the current and previous measurement sets ξ. This distribution will be estimated recursively as a Bayes filter, as it is equivalent to $p(\hat{\Lambda}_k|\hat{\Lambda}_{k-1}, \xi_k)$ using the Markov assumption [19]. This distribution is expected to be multimodal, so will be described as a sum of L Gaussian components ρ given by

$$p(\hat{\Lambda}_k|\hat{\Lambda}_{k-1}, \xi_k) = \sum_{l=1}^{L} a_l \rho_l = \sum_{l=1}^{L} a_l \mathcal{N}(\lambda_l, v_l) \tag{15}$$

each with a weighting $a_l = L^{-1}$, a mean λ_l, and variance v_l. L varies as described in Algorithm 1. This probability distribution is illustrated in Fig. 4. The distribution is updated using the following three steps, with Algorithm 1 described in Fig. 5.

1) Data association is found between the measurements ξ_k and each of the components ρ_l, using a similar measure to that in Equation 10. If a match is found with an existing component, the component mean and variance are updated using the computed Kalman gain similarly to Equations 11 to 13. This is equivalent to calling Algorithm 1 with parameters $\zeta = \xi_k$, $\alpha = 1$, and $\beta = 1$.
2) The static measurements will result in a number of components at integer multiples of the pipe length due to higher order echoes. Therefore, integer fractions of each of the components $(\frac{1}{2}\lambda_l, \frac{1}{3}\lambda_l, \dots)$ can be fused with the other components. This is equivalent to calling Algorithm 1 with parameters $\zeta = \{\frac{1}{2}\lambda, \frac{1}{3}\lambda, \dots\}$, $\alpha = 0.5$, and $\beta = 0$.

Algorithm 1: Pipe Length Kalman Filter Update

procedure UPDATE($\lambda_k, v_k, L, Q_k, \zeta, \alpha, \beta$)
  for each ζ_n in ζ **do**
    Get data association π:
    for each [λ_l, v_l] pair in λ_k and v_k **do**
      $\Psi_{ln} = v_l + Q_k$
      $\pi_{ln} = (\zeta_n - \lambda_l)^2 \Psi_{ln}^{-1}$
    end for
    if min $\pi_n < \alpha$ **then**
      Do Kalman update:
      $j = \arg\min_l \pi_n$
      $K_i = v_l \Psi_{ln}^{-1}$
      $\lambda_{jk} = \lambda_{jk} + K_i(\zeta_n - \lambda_{jk})$
      $v_{jk} = (1 - K_i) v_{jk}$
    else
      Create new component:
      if β = 1 **then**
        $L = L + 1$
        $\lambda_{Lk} = \zeta_n$
        $v_{Lk} = Q_k$
      end if
    end if
  end for
  return λ_k, v_k, L
end procedure

Fig. 5. The algorithm used to update the probability distribution over possible pipe lengths Λ given input measurements or virtual measurements ζ. The data association and Kalman filter updates are the equivalent of Equations 9 to 13 in a slightly different form since the variables are all scalar rather than vectors.

3) The current set of components can be consolidated, combining similar measurements, equivalent to calling Algorithm 1 with parameters $\zeta = \lambda_k$, $\alpha = 2$, and $\beta = 0$, and removing one of the components if a match is found, reducing L and reindexing λ_k.

To infer an estimate of pipe length from $p(\hat{\Lambda}_k | \hat{\Lambda}_{k-1}, \xi_k)$ seen in Fig. 4, the peaks of each Gaussian component are compared to a threshold probability. If the largest peak is sufficiently higher than the second largest peak, its mean value is used as the pipe length estimate $\hat{\Lambda}_k$. Measurements $\xi_{n,k}$ similar to multiples of $\hat{\Lambda}_k$ according to a comparison

$$\gamma > |\xi_{n,k} - a\hat{\Lambda}_k| \tag{16}$$

for $a = (1, 2, 3, \ldots)$ where γ is a threshold, can be removed from ξ_k. $\hat{\Lambda}_k$ can be used as a virtual measurement between map features p_m as in Equation 14.

III. RESULTS

In this section, the localization method is evaluated over 50 trajectories and over a range of parameters for measurement uncertainty. This is done using simulations based on experimental data which has been recorded for 11 positions along a 15 metre pipe at 0.5 metre intervals, giving impulse responses such as those shown in Fig. 2(d).

Synthetic measurement sets ξ_k can be created using this data to allow simulation of any robot trajectory through the pipe. Evaluation of the front-end acoustic processing in section II-B showed that the measurement output distances ξ_k are well modelled as normally distributed additive noise on the true distance, with a mean of zero and a variance of 0.09 metres.

The Kalman filter based methods are compared here to a *dead reckoning* method which simply integrates the command motion of the robot, and a simple *measurement-only* method, which uses either the first or second (denoted by (1) and (2) respectively) value in the measurement set ξ_k as the position of the robot relative to the starting position.

Fig. 6 shows a comparison of these different estimation methods over a complete trajectory along the length of the pipe. The dead reckoning estimate is seen to drift considerably. The simple estimates using only the instantaneous measurements are seen to be reasonably accurate over half of the trajectory each, but completely incorrect otherwise. The Kalman filter estimated position is seen to be consistent along the full trajectory, with a lower error when $\hat{\Lambda}_k$ is incorporated.

To investigate the robustness of the localization method, the synthetic measurement sets can be modified, either adding spurious measurements or removing measurements, modelling errors that may occur in acoustic signal processing. At each time step, a number of measurements drawn from a uniform distribution from 0 to θ_s or θ_m is added or removed respectively from the set ξ_k. The measurements added are a product of random variables, defined by $U(0, \frac{15}{2})U(0, \frac{15}{2})$ where $U(0, \frac{15}{2})$ is a uniform distribution between 0 and half the pipe length, used to produce values which are more likely to interfere with first-order echoes.

Fig. 7 shows the sensitivity of the localization method to spurious or missing measurements over a range of values of parameters θ_s and θ_m. Similar trends are seen for increase of both parameters. The error for *measurement-only* estimation (using the closer of the two estimates, assuming that it can be correctly chosen) is seen to increase with both parameters, surpassing the benchmark dead-reckoning error,

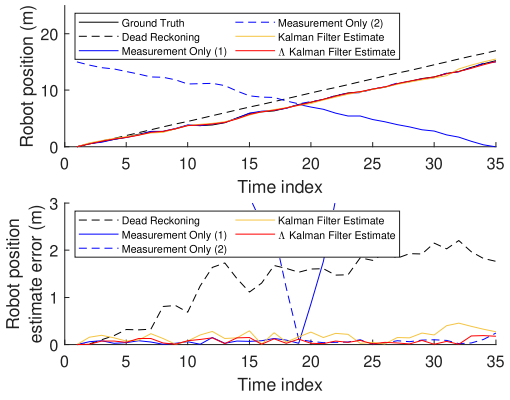

Fig. 6. The estimate of robot position over time as it moves through a 15 metre long pipe. The true robot position is estimated well by the Kalman filter output, which gives much lower estimate error than the dead-reckoning estimate. The estimates using measurement only give low error, but only for half of the trajectory as filtering is needed to determine the direction of the acoustic measurements made using only one microphone.

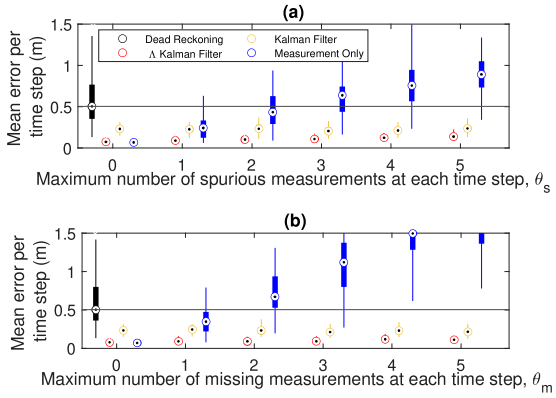

Fig. 7. An analysis of the sensitivity of the localization to spurious (a) or missing (b) measurements. A random number of measurements are added or removed from the measurement set at each time step. The quartile results over 50 simulated trajectories through a pipe are given using box plots. The dead-reckoning estimate remains unchanged, as a benchmark. The measurement only result uses the lowest error of the two measurements, giving a best case for comparison. The Kalman filter estimate with an without the use of the pipe length estimate is shown.

showing the need for filtering. The use of the Kalman filter using only measurements ξ_k is shown to keep the median estimate error at a constant value, however it is larger than the *measurement-only* estimate for zero missing or spurious measurements. Incorporating $\hat{\Lambda}_k$ into the Kalman filter is shown to reduce the error further, and this estimate is seen to be only slightly sensitive to the increase in parameters.

As expected, the use of acoustic echoes at direct measurements of the robot's state is effective for localization. The algorithm proves to be robust to a significant number of measurement errors, showing promise for practical application. The use of the estimated pipe length is seen to give a surprising increase in accuracy, and similar uses of the known structure of the environment may be useful in other applications of acoustic localization.

The localization approach may be improved further by using a smoothing approach rather than a filtering approach. By estimating the full robot trajectory along the pipe rather than the instantaneous position of the robot, spurious measurements can be more easily detected and removed before they influence the estimation.

IV. CONCLUSIONS

This paper has presented a complete acoustic echo-localization method, from acoustic processing to state estimation, for a robot moving along a pipe. A novel means of estimating the echo class from the acoustic data has been presented and demonstrated, which allows refinement of the acoustic measurements before state estimation, reducing the estimation error. The robustness of the method to spurious and missing feature measurements has been demonstrated. The presented method would give a useful input to sensor fusion filtering, which might be improved by using a smoothing approach to allow easier detection of spurious measurements.

ACKNOWLEDGMENT

We acknowledge funding support from EPSRC grant EP/S016813/1 Pervasive Sensing for Buried Pipes (Pipebots), and the support and advice from Kirill Horoshenkov and EPSRC grant EP/N010124/1, TWENTY 65: Tailored Water Solutions for Positive Impact.

REFERENCES

[1] B. Park, "Resilient Underground Localization Using Magnetic Field Anomalies for Drilling Environment," *IEEE Transactions on Industrial Electronics*, vol. 65, no. 2, pp. 1377–1387, 2018.

[2] H. Najjaran and D. Krys, "INS-ASSISTED MONOCULAR ROBOT LOCALIZATION," *Proceedings of the ASME 2010 International Mechanical Engineering Congress & Exposition*, pp. 1–8, 2010.

[3] P. Hansen, H. Alismail, B. Browning, and P. Rander, "Stereo visual odometry for pipe mapping," *IEEE International Conference on Intelligent Robots and Systems*, pp. 4020–4025, 2011.

[4] P. Hansen, H. Alismail, P. Rander, and B. Browning, "Pipe mapping with monocular fisheye imagery," *IEEE International Conference on Intelligent Robots and Systems*, pp. 5180–5185, 2013.

[5] A. Kakogawa, Y. Komurasaki, and S. Ma, "Anisotropic shadow-based operation assistant for a pipeline-inspection robot using a single illuminator and camera," *IEEE International Conference on Intelligent Robots and Systems*, vol. 2017-Septe, pp. 1305–1310, 2017.

[6] W. Zhao, M. Kamezaki, K. Yoshida, M. Konno, A. Onuki, and S. Sugano, "Modeling and simulation of FLC-based navigation algorithm for small gas pipeline inspection robot," *IEEE/ASME International Conference on Advanced Intelligent Mechatronics, AIM*, vol. 2018-July, pp. 912–917, 2018.

[7] H. Lim, J. Y. Choi, Y. S. Kwon, E.-j. Jung, and B.-j. Yi, "SLAM in Indoor Pipelines with 15mm Diameter," *Int. Conf. on Robotics and Automation, pp. 4005-4011.*, pp. 4005–4011, 2008.

[8] A. C. Murtra and J. M. Mirats Tur, "IMU and cable encoder data fusion for in-pipe mobile robot localization," *IEEE Conference on Technologies for Practical Robot Applications, TePRA*, pp. 1–6, 2013.

[9] W. M. Al-Masri, M. F. Abdel-Hafez, and M. A. Jaradat, "Inertial Navigation System of Pipeline Inspection Gauge," *IEEE Transactions on Control Systems Technology*, vol. PP, pp. 1–8, 2018.

[10] K. Ma, M. Schirru, A. H. Zahraee, R. Dwyer-Joyce, J. Boxall, T. J. Dodd, R. Collins, and S. R. Anderson, "PipeSLAM: Simultaneous Localisation and Mapping in Feature Sparse Water Pipes using the Rao-Blackwellised Particle Filter," *IEEE/ASME International Conference on Advanced Intelligent Mechatronics, AIM*, pp. 1459–1464, 2017.

[11] T. Seco, C. Rizzo, J. Espelosín, and J. L. Villarroel, "A Robot Localization System Based on RF Fadings Using Particle Filters inside Pipes," *Proceedings - 2016 International Conference on Autonomous Robot Systems and Competitions, ICARSC 2016*, pp. 28–34, 2016.

[12] Y. Bando, H. Suhara, M. Tanaka, T. Kamegawa, K. Itoyama, K. Yoshii, F. Matsuno, and H. G. Okuno, "Sound-based online localization for an in-pipe snake robot," *SSRR 2016 - International Symposium on Safety, Security and Rescue Robotics*, pp. 207–213, 2016.

[13] C. Evers, S. Member, P. A. Naylor, and S. Member, "Acoustic SLAM," *IEEE/ACM Transactions on Audio, Speech, and Language Processing*, vol. 26, no. 9, pp. 1484–1498, 2018.

[14] M. Krekovic, I. Dokmanic, and M. Vetterli, "EchoSLAM : Simultaneous Localization and Mapping with Acousitc Echoes," *2016 IEEE International Conference on Acoustics, Speech and Signal Processing (ICASSP)*, pp. 11–15, 2016.

[15] M. Krekovic, I. Dokmanic, and M. Vetterli, "Look, no Beacons! Optimal All-in-One EchoSLAM," 2016. [Online]. Available: http://arxiv.org/abs/1608.08753

[16] U. Saqib and J. R. Jensen, "Sound-based distance estimation for indoor navigation in the presence of ego noise," *European Signal Processing Conference*, vol. 2019-Septe, pp. 1–5, 2019.

[17] J. Mourjopoulos, "On the variation and invertibility of room impulse response functions," *Journal of Sound and Vibration*, vol. 102, no. 2, pp. 217–228, 1985.

[18] D. Salvati, C. Drioli, and G. L. Foresti, "Sound Source and Microphone Localization from Acoustic Impulse Responses," *IEEE Signal Processing Letters*, vol. 23, no. 10, pp. 1459–1463, 2016.

[19] S. Thrun, W. Burgard, and D. Fox, *Probabilistic Robotics*. The MIT Press, 2006.